Preprints of the 10th IFAC International Symposium on Dynamics and Control of Process Systems
The International Federation of Automatic Control
December 18-20, 2013. Mumbai, India

Multivariate Image and Texture Analysis for Film-Coated Tablets Elegance Assessment

Matteo Ottavian*. Massimiliano Barolo.*
Salvador García-Muñoz**

**CAPE-Lab – Computer-Aided Process Engineering Laboratory, Department of Industrial Engineering, University of Padova, via Marzolo 9 – 35131 Padova, Italy (e-mail: max.barolo@unipd.it).*
***Pfizer Worldwide Research & Development,*
445 Eastern Point Road, Groton (CT), USA (e-mail:sal.garcia@pfizer.com)

Abstract: The use of multivariate image and texture analysis is proposed in this study to quantitatively characterize the elegance of film-coated tablets. Four unsupervised metrics are developed to quantify both the color uniformity of tablet faces/bands and the erosion level inside and outside the tablet logo. Latent variable modeling is used to regress the measured elegance against coating operating conditions in order to investigate the driving forces acting on the system, consistently with the quality-by-design framework promoted by the Food and Drug Administration.

Keywords: image analysis; tablet coating; tablet elegance; multivariate data analysis; quality by design

1. INTRODUCTION

The Food and Drug Administration (2006) has been encouraging the design and validation of pharmaceutical processes within a multidimensional domain of processing conditions, referred to as the process design space. Within the chosen design space, pharmaceutical companies should provide evidence that the resulting product is acceptable, being safety and efficacy the foremost priority. This concept is referred to as Quality by Design. The proposed design space has to be supported by the scientific understanding of the driving forces acting on the system and governing the complex network of interactions between materials, process and product. This framework should be based on metrics that are robust and reproducible, and not on qualitative ones that might be easily biased by human perception (García-Muñoz and Carmody, 2010).

Film coating is a common processing step in the manufacture of tablets (Libermen et Lachman, 1981). Tablets are loaded inside a rotating pan and sprayed with an aqueous or non-aqueous solution, and air is used to evaporate the solvent. Tablet coating is carried out for several reasons. It can enhance the tablet stability, because the core might contain a substance that is not compatible with light and/or subject to atmospheric oxidation. Also tablet mechanical integrity (i.e., higher resistance to mishandling) can be enhanced by coating. Furthermore, coating can cover a bitter taste or an unpleasant odor of a substance within the tablet core, or it can modify the drug release profile (e.g., enteric coating, osmotic pump, pulsatile delivery; Libermen et Lachman, 1981; Cole et al., 1995).

The elegance of film-coated tablets have been usually related to color uniformity and surface finish (roughness/erosion), and several techniques have been proposed for its characterization (Ruotsalainen et al., 2003; Seitavuopio et al., 2006). Among them, the use of multivariate image (MIA) and wavelet texture analysis (MWTA) has been suggested by García-Muñoz and Gierer (2010) and García-Muñoz and Carmody (2010). Both MIA and MWTA rely on simple color images taken with a digital camera, which is much less expensive and easier to operate than other equipment. Hence, the use of MIA and MWTA is attractive for practical industrial applications, where the elegance assessment is still typically performed by a trained panel of experts and, as such, may suffers from reproducibility issues.

In this paper, MIA and MWTA are combined together to quantify the elegance of film-coated tablets through several indices with the aim of supporting pharmaceutical manufacturing. The proposed strategy is applied to multiple batches of tablets coated at different conditions. Projection to latent structures (PLS; Geladi and Kowalski, 1986) is used to regress the measured elegance against the coating operating parameters, in order to investigate the main driving forces of the process.

The paper is organized as follows. Section 2 presents the experimental apparatus and the available data. Section 3 provides an overview of the multivariate data analysis techniques used throughout the paper. Sections 4 and 5 describe the unsupervised metrics defined for elegance assessment. These metrics are regressed against process operating conditions in Section 6.

2. IMAGING STATION AND AVAILABLE DATA

The in-house imaging station used in this study was equipped with a digital single-lens reflex Canon EOS 40D camera (10.1 megapixel resolution) with a Canon EF-S 60 mm f/2.8 USM Macro lens. LED lights illuminated the subjects (two racks mounting 64 LEDs each), and the system was isolated from the outside and operated through a computer. The user was allowed to set camera elevation, lights elevation (hence changing the angle of incidence of the light on the subject surface) and camera settings (used to ensure proper exposure). Images were collected off-line for five different batches, indicated as Batches A-E. For color uniformity assessment, the tablets were withdrawn from the coater during the coating process, and tablet faces and bands were imaged separately. Several tablets were photographed per each single image; furthermore, three images of faces and three images of bands were taken for each pull point. For erosion assessment, the tablets were imaged at the end of the coating process (one tablet per image), using an angle of incidence of the light onto the tablets surfaces that allowed to highlight the defects (if any). Details on the number of images collected for each batch are given in Table 1.

Table 1. Images collected for each batch.

Batch	Number of pull point (color uniformity)	Number of tablets (erosion analysis)
A	4	1308
B	6	1142
C	7	994
D	6	765
E	6	1148

Batches A-E were characterized by different operating conditions (in terms of batch duration, spray rate, pan load and rotation speed) and tablets formulation details (particularly tablets hardness). A detailed list of process operating conditions is given in Table 2.

Table 2. Film coating operating parameters.

Variable name	Description
Duration 1	Phase 1 duration
Exhaust T1	Phase 1 exhaust air temperature
Spray 1	Phase 1 spray rate
Duration 2	Phase 2 duration
Spray 2	Phase 2 spray rate
Pan load	Amount of loaded tablets
Pan speed	Pan rotational speed
Hardness	Average tablets hardness

It should be noticed that the coating process was run in two phases, exploring different duration /spray rate combinations. The air flowrate and the exhaust temperature of the second phase were kept constant (the latter by adjusting the inlet air temperature), and hence they do not appear in Table 2. It should be stressed that other variables that might have affected either the coating uniformity or the surface erosion (gun to bed distance, air pressure, etc.; Cole et al., 1995; García-Muñoz and Carmody, 2010) were not changed in the batches considered in the present study, and hence they did not represent a source of variability to include in the models.

3. METHODS

3.1 Principal component analysis

Given a generic matrix $\mathbf{X}$ $[N\times M]$, its principal component analysis (PCA; Jackson, 1991) decomposition is given by

$$\mathbf{X} = \mathbf{T}\mathbf{P}_{\mathrm{PCA}}^{\mathrm{T}} + \mathbf{E}_{\mathbf{X}} \tag{1}$$

with $\mathbf{T}$ $[N\times A]$, $\mathbf{P}_{\mathrm{PCA}}$ $[M\times A]$ and $\mathbf{E}_{\mathbf{X}}$ $[N\times M]$ being respectively the scores, loadings and residual of the model built on A principal components (PCs), and the superscript $^{\mathrm{T}}$ indicating the transpose of a matrix. Note that the data in $\mathbf{X}$ need to be properly scaled before transformation (1) is carried out. PCA summarizes the information stored in the $\mathbf{X}$ matrix by defining a low-dimensional space (called latent space), whose axes (of which the A loadings are the direction cosines) represent the directions of maximum variability of the original data. The scores $\mathbf{T} = [\mathbf{t}_1, \mathbf{t}_2, \ldots, \mathbf{t}_A]$ are the projections of $\mathbf{X}$ onto the latent space. They represent the new variables, and are orthogonal to each other.

3.2 Projection to latent structures

Given a matrix $\mathbf{Y}$ $[N\times I]$ of I quality (or response) indicators of the N samples of $\mathbf{X}$, a PLS model (Geladi and Kowalski, 1986) finds the driving forces that are most related to the response, by maximizing the correlation among the projections of $\mathbf{X}$ and $\mathbf{Y}$ onto a common latent space (the model space). Formally,

$$\mathbf{X} = \mathbf{T}\mathbf{P}_{\mathrm{PLS}}^{\mathrm{T}} + \mathbf{E}_{\mathbf{X}} \tag{2}$$

$$\mathbf{Y} = \mathbf{T}\mathbf{Q}^{\mathrm{T}} + \mathbf{E}_{\mathbf{Y}} \tag{3}$$

$$\mathbf{T} = \mathbf{X}\mathbf{W}^{*} \tag{4}$$

where $\mathbf{P}_{\mathrm{PLS}}$ $[M\times A]$ and $\mathbf{Q}$ $[I\times A]$ are the loadings relating the projections in the model space $\mathbf{T}$ to the data matrices $\mathbf{X}$ and $\mathbf{Y}$ (respectively). $\mathbf{W}^{*}$ $[M\times A]$ is the weight matrix, through which the data in $\mathbf{X}$ are projected onto the latent space to give the scores $\mathbf{T}$. $\mathbf{E}_{\mathbf{X}}$ $[N\times M]$ and $\mathbf{E}_{\mathbf{Y}}$ $[N\times I]$ are the residual matrices, and account for the mismatch in the reconstruction of the original data. Both $\mathbf{X}$ and $\mathbf{Y}$ data need to be scaled prior to being transformed through PLS. The relative importance of each predictor within the PLS model can be evaluated through a modified variable importance in projection (VIP) index, which is defined for variable m as

$$\mathrm{VIP}_m = \frac{\sum_{a=1}^{A} w_{ma}^{*2} \cdot R_a^2\mathbf{Y} \cdot M}{R^2\mathbf{Y}} \tag{5}$$

being w_{ma}^{*} the weight of the m-th variable on the a-th component and $R^2_a\mathbf{Y}$ and $R^2\mathbf{Y}$ the explained variance of the response matrix, respectively for the a-th LV and for the overall PLS model.

3.3 Multivariate image analysis

Multivariate image analysis (MIA; Prats-Montalbán et. al., 2011) relies on the PCA decomposition of an image. RGB images (such as those available in this study) are three-way arrays of size $[N_{row}\times N_{col}\times 3]$, whose first two dimensions are the number of pixel rows (N_{row}) and columns (N_{col}). The third dimension represents the light intensity along the red (R), green (G) and blue (B) channels, and is a value bounded within the range [0-255]. Prior to the PCA factorization to generate two scores vectors ($\mathbf{t}_1$ and $\mathbf{t}_2$), images are unfolded into two-way matrices of size $[(N_{row} \cdot N_{col}) \times 3]$, as depicted in Figure 1 for a sample image.

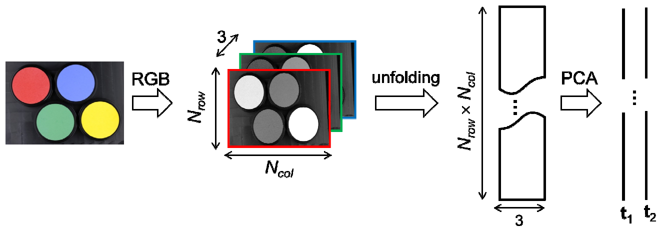

Fig. 1. Schematic of multivariate image analysis (MIA).

The $\mathbf{t}_1$ and $\mathbf{t}_2$ scores (which typically account for more than 90% of the total variability on $\mathbf{X}$) are scaled within the range [0-255]. The score space is usually represented in terms of a two dimensional (2D) histogram-scatter (or density) plot, as shown in Figure 2 for the image of Figure 1 (the color in Figure 2a is related to the number of pixels having specified $\mathbf{t}_1$ and $\mathbf{t}_2$ coordinates; i.e. the lighter the color, the larger the number of pixels). Pixels having projections close to each other in the score space are similar in terms of color structure, regardless of their spatial arrangement in the original image. This can be easily seen by defining a *mask* (i.e. a geometrical shape highlighting a certain region of the $\mathbf{t}_1\mathbf{t}_2$ space) and looking at the pixels in the original image that project within it. An example is given in Figure 2a, where the mask is used to highlight the red pixels in the original image.

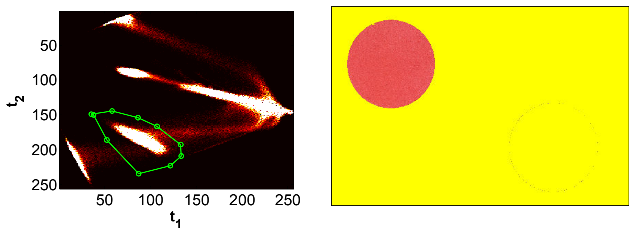

(a) (b)

Fig. 2. (a) 2D histogram-scatter plot of the score space of the MIA model built on the image of Figure A1, with a mask defined on it (green contour). (b) pixels (in the original image) whose projection lay underneath the mask defined in (a).

The 2D histogram-scatter plot is the starting point for covariance mask method (García-Muñoz and Gierer, 2010) used in this work in the definition of the color uniformity metrics

3.4 Multivariate texture analysis

Multivariate texture analysis by means of the wavelet transform (MWTA; Duchesne et al., 2012) is considered to be state-of-the-art among other texture analysis methods (Liu and Han, 2011). MWTA relies on the discrete wavelet transform (Addison, 2002), which decomposes a bi-dimensional signal (such as an image) into a sequence of approximations (low-resolution elements, $\mathbf{A}$) and details (high-resolution elements, $\mathbf{D}$) through the convolution with low-pass and high-pass filters, hence returning a multi-resolution representation of the original data. Texture-related information are typically stored within the details, whose information at each decomposition stage k can be summarized with a synthetic descriptor such as the energy E, defined as

$$E_k = \left\| \mathbf{D}_k \right\|_{\mathrm{F}}^2 \tag{5}$$

where $\left\| \cdot \right\|_{\mathrm{F}}$ denotes the Frobenius norm. Thus, for each image, a feature vector of size $[1 \times K]$ can be extracted, being K the number of decomposition scales retained.

4. COLOR UNIFORMITY ASSESSMENT

The color signature introduced by García-Muñoz and Gierer (2010) was used to characterize the tablet color uniformity. The color signature is an unbiased metric that evolves as long as coating material is applied to the tablets, until a certain end-point is reached. For each lot of tablets, the following procedure was used (García-Muñoz and Gierer; 2010):

1. calibration of an MIA model on the composite image obtained from the concatenation of all the images available for the lot;
2. background removal, by fitting a second PCA model on the scores obtained from the projection of some background images onto the MIA model;
3. manipulation of the 2D histogram-scatter plots according to the covariance mask method (Yu and MacGregor, 2003), using the time of each withdrawn as the dependent variable;
4. calibration of a 1-PC PCA model on the matrix obtained by stacking on the top of each the features vectors extracted from the 2D histogram-scatter plots, the score $\mathbf{t}_1$ representing the color signature;
5. application of the covariance mask and of the PCA model defined in steps 3 and 4 (respectively) to the scores resulting from the projection of the sub-images (approximately of the size of one tablet) extracted from each available image on the MIA model of step 1.

The last step allowed to extract the color signature for both tablets faces and bands (separately), as shown in Figure 3 for one of the five available batches.

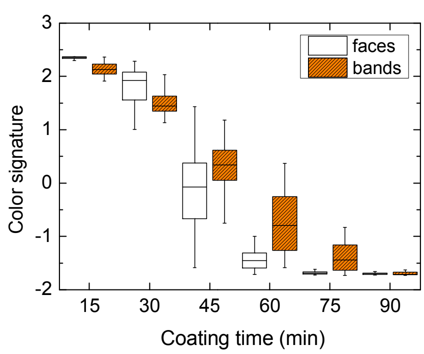

Fig. 3. Color signature evolution of faces (open boxes) and bands (hashed boxes) for Batch D.

Results for all lots are summarized in Figure 4 in terms of range of the color signature distribution at each withdrawal (difference between the two extreme values) versus the percentage of the coating operation completed (withdrawal time divided by the total batch time), in such a way that all lots are scaled to a 0-100% *x*-axis. To avoid including potential outliers in the result, the interquartile range (25^{th} – 75^{th} percentiles) was used. Figure 4 highlights that bands require longer coating time than faces, because the peaks of the distributions are shifted to higher fractions of the completion time. In fact, although the end-point is the same (cf. Fig. 3), the color signature range of faces reaches its lowest value at around 75% of the total batch time, whereas for bands it evolves until the end of the batches.

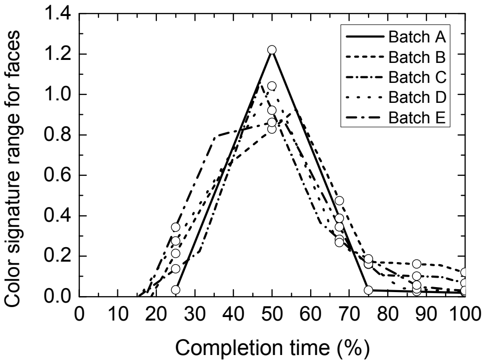

(a)

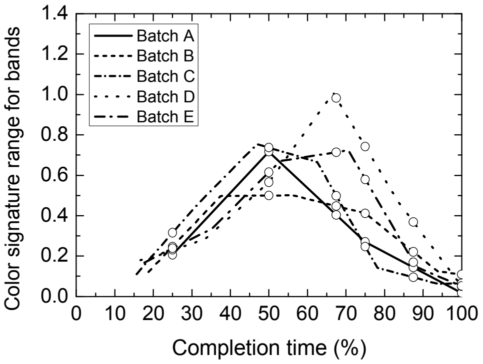

(b)

Fig. 4. Color signature range evolution for (a) faces (b) and bands for Batches A-E.

5. EROSION ASSESSMENT

The application of MWTA for erosion quantification required several preprocessing steps on the images prior to the analysis, in order to perfectly align and properly cut all tablets images to the greatest area around the logo. The preprocessing operations were automated: tablets were localized within each image by using the derivative of the summation of the grayscale intensities along the two spatial directions, while the cropping operation involved simple trigonometric calculations (García-Muñoz and Carmody, 2010). After cropping, images of tablets surfaces were converted to grayscale. An example of two tablet surfaces characterized by a different level of erosion is given in Figure 5.

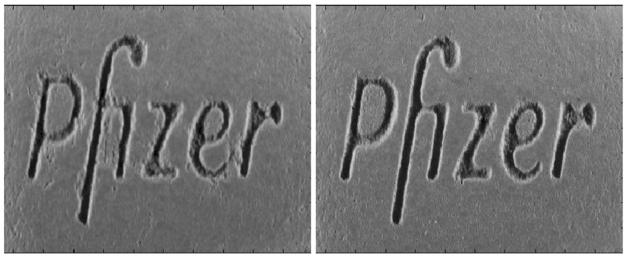

(a) (b)

Fig. 5. Examples of two different tablet surfaces characterized by different erosion level: tablet (a) is more eroded than tablet (b).

With respect to the images of Figure 5, texture analysis was complicated by the presence of the logo. As suggested by Russ (1999), texture can be defined as a descriptor of local brightness variation from pixel-to-pixel in a small neighborhood. Hence, texture analysis was found to be biased towards the detection of the logo, since it localizes the greatest pixel-to-pixel brightness variations. For this reason, the erosion quantification exercise was split into two separate problems, i.e. the erosion quantification inside and outside the logo. A template matching technique (Lewis, 1995) was used to extract the logo from each image. The metrics developed to quantify the erosion inside and outside the logo are presented in the following sections.

5.1 Inside logo erosion assessment

The erosion quantification inside the logo relied on the consideration that the darker the logo, the easier to read it, since erosion does not affect it. Hence, the light intensity distribution of the logo pixels (i.e. the distribution of the values of the light intensity for each pixel) was used to characterize each tablet. In order to develop a synthetic descriptor of the erosion inside the logo (which will be indicated as "logo index" hereafter), the following procedure was used:

1. for each lot, evaluation of the average light intensity distribution;
2. calibration of a 1-PC PCA model on the matrix built from the average light intensity distributions, the score t1 being the average logo index for the batch;
3. for each lot, projection of the light intensity distribution of each tablet onto the PCA model, generating a $\mathbf{t}_1$ distribution.

The logo index distributions of the five batches are given in Figure 6. Higher values of the logo index indicate higher (average) erosion of the logo. Figure 6 suggests that Batches B and C are characterized by a higher erosion level than the other batches.

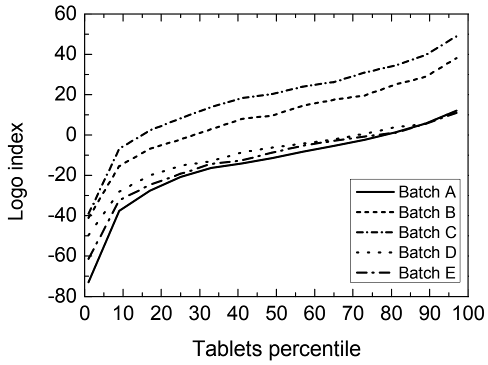

Fig. 6. Logo index distributions for Batches A-E.

5.2 Outside logo erosion assessment

Erosion outside the logo was evaluated by means of the wavelet transform using the Coiflets 5 wavelet (Addison, 2002). Only the details at the fourth decomposition stage were considered, since higher stages extracted useless information. Figure 7 shows the details at the fourth decomposition stage for the tablets of Figure 5.

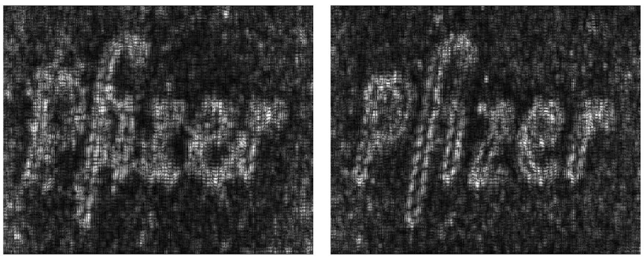

(a) (b)

Fig. 7. Fourth decomposition stage wavelet details for the tablets of Figure 5.

Pixels highlighted in white in Figure 7 identify the discontinuities in the tablets surfaces. Thus, the lighter the detail image, the higher its energy index (E_4), the more eroded the tablet. For the computation of the energy index, pixels belonging to the logo were excluded.

Each of the five batches was characterized by an energy distribution. Results are shown in Figure 8.

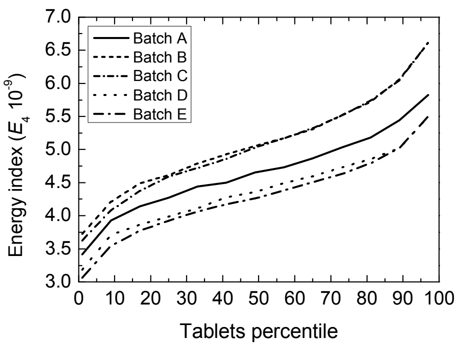

Fig. 8. Energy index distributions for Batches A-E.

Figure 8 returns results similar to those of Figure 6, i.e. Batches B and C are those characterized by a higher erosion level.

6. REGRESSING ELEGANCE METRICS AGAINST COATING OPERATING CONDITIONS

The four elegance metrics defined in Sections 4-5 were used to build the quality matrix **Y** to be regressed against the [5×8] **X** regressor matrix (the coating operating conditions listed in Table 2). Namely, **Y** was defined as $\mathbf{Y} = [\mathbf{Y}_{\text{faces}}\ \mathbf{Y}_{\text{bands}}\ \mathbf{Y}_{\text{logo}}\ \mathbf{Y}_{\text{energy}}]$, i.e. **Y** was obtained from the horizontal concatenation of the color signature range of faces ($\mathbf{Y}_{\text{faces}}$ [5×6]) and bands ($\mathbf{Y}_{\text{bands}}$ [5×6]), the erosion logo index ($\mathbf{Y}_{\text{logo}}$ [5×13]) and the energy index ($\mathbf{Y}_{\text{energy}}$ [5×13]) . Prior to the concatenation into **Y**, however, the matrices of the four metrics were further simplified:

- $\mathbf{Y}_{\text{logo}}$ and $\mathbf{Y}_{\text{energy}}$ were reduced to [5×3] matrices considering the high correlation among the variables (verified using a PCA model); only the first, mid and last points of each distribution were retained;
- $\mathbf{Y}_{\text{faces}}$ and $\mathbf{Y}_{\text{bands}}$ were reduced to a [5×2] matrix and a [5×1] matrix respectively, retaining only the last points of the distributions; in fact, the appropriate color uniformity needs to be ensured only at the end of the coating process.

The diagnostics of the 3-LV PLS model relating **X** and **Y** are given in Table 3 in terms of coefficient of determination per component (R^2) and cumulated (R^2_{CUM}) for both the predictor and the response matrices. While 2 LVs were probably sufficient to explain quality, the third LV was included in the model since it greatly contributed in the definition of the **X** space (Tomba et al., 2012).

Table 3. PLS model diagnostics.

LV	$R^2\mathbf{X}$	$R^2_{\text{CUM}}\mathbf{X}$	$R^2\mathbf{Y}$	$R^2_{\text{CUM}}\mathbf{Y}$
1	52.6	52.6	64.7	64.7
2	20.9	73.5	19.6	84.3
3	25.3	98.8	8.70	93.0
4	1.20	100	7.00	100

The PLS scores, loadings and modified variable importance in projection (VIP) index are shown in Figure 9.

The score plot (Figure 9a) clearly clusters batches B and C at negative $\mathbf{t}_1$ values. Recall that these batches are characterized by poor surface finish. The $\mathbf{W}^*/\mathbf{Q}$ biplot (Figure 9b) clarifies the main driving forces of the process and product characteristics and how they relate to the erosion of the product. The obvious relationships in the plot lead to conclude that higher hardness and pan-speed leads to less erosion, and that the larger the duration of the phases, the more erosion the tablets will exhibit. It is interesting to observe that the spray rate and the thermodynamic conditions of the coater do not have an obvious and direct effect onto the overall erosion. This is seen also in the modified VIP index (Figure 9c), where the predictors are ranked according to their importance within the PLS model.

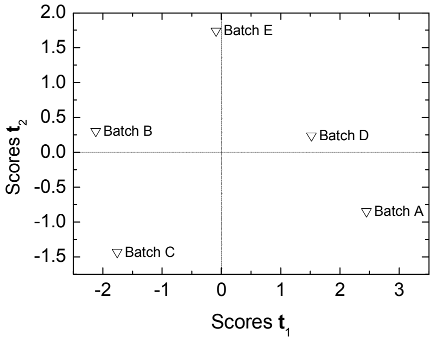

(a)

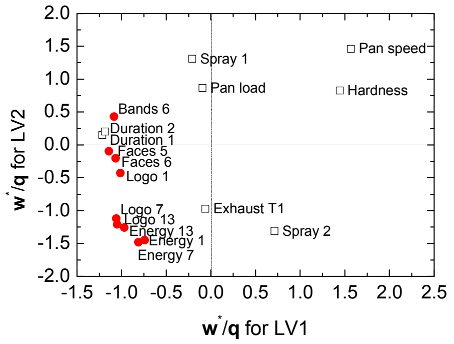

(b)

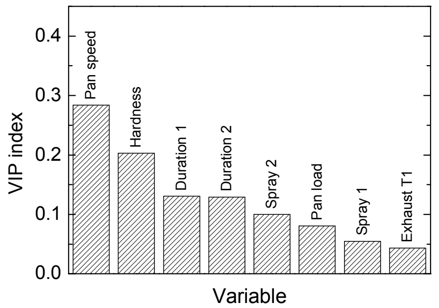

(c)

Fig. 9. PLS model (a) scores, (b) loadings biplot and (c) modified VIP index.

Based on the PLS model results, some recommendations could be obtained on how to run the film coating process. Batches A and D, in fact, returned the best overall tablets elegance, as suggested by the combined analysis of the $\mathbf{t}_1\mathbf{t}_2$ plot (Figure 9a) and of the $\mathbf{W}^*/\mathbf{Q}$ biplot (Figure 9b).

7. CONCLUSIONS

This paper presented the use of multivariate image and texture analysis for the assessment of film coated tablets elegance. The regression of the elegance metrics against the coating operating conditions allowed to investigate the process design space. Recommendations on how to run the film coating operation were given based on the diagnostics of the regression model. More sophisticated approaches, based on the concept of latent variable model inversion (Tomba et al., 2012), will be investigated in the future in order to properly optimize the process.

REFERENCES

Addison, P.S. (2002). *The Illustrated Wavelet Transform Handbook*. Taylor & Francis, New York (USA).

Cole, G., Hogan, J.E. and Aulton, M.E. (1995). *Pharmaceutical coating technology*. Taylor and Francis, London (UK).

Duchesne, C., Liu, J.J. and MacGregor, J.F. (2012). Multivariate image analysis in the process industry: a review. *Chemom. Intell. Lab. Syst.*, 117, 116-128.

Food and Drug Administration (2006). Guidance for industry, quality system approach to pharmaceutical CGMP regulations. Pharmaceutical CGMPs.

García-Muñoz, S. and Carmody, A. (2010). Multivariate wavelet texture analysis for pharmaceutical solid products characterization. *Int. J. Pharm.*, 398, 97-106.

García-Muñoz, S. and Gierer, D. (2010). Coating uniformity assessment for colored immediate release tablets using multivariate image analysis. *Int. J. Pharm.*, 395, 104-113.

Geladi, P. and Kowalski, R. (1986). Partial least squares regression: a tutorial. *Anal. Chim. Acta*, 185, 1-17.

Jackson, J.E. (1991). *A user's guide to principal components*. John Wiley & Sons, New York (USA).

Lewis, J.P. (1995). Fast template matching. Vision Interface 95, Canadian Image Processing and Pattern Recognition Society, Quebec City, Canada, May 15-19, 120-123.

Libermen, H. and Lachman, L. (1981). *Pharmaceutical dosage forms: tablets*. Marcel Dekker Inc., New York (USA).

Liu, J.J., and Han, C. (2011). Wavelet texture analysis in process industries. *Korean J. Chem. Eng.*, 28, 1814-1823.

Prats-Montalbán, J.M., de Juan, A. and Ferrer, A. (2011). Multivariate image analysis: a review with applications. *Chemom. Intell. Lab. Syst.*, 107, 1-23.

Ruotsalainen, M., Heinämäki, J., Guo, H., Laitinen, N. and Yliruusi, J. (2003). A novel technique for imaging film coating defects in the film-core interface and surface of coated tablets. *Eur. J. Pharm. Biopharm.*, 56, 381-388.

Russ, J.C. (1999). *The Image Processing Handbook*. CRC Press, Florida (USA).

Seitavuopio, P., Heinämäki, J., Rantanen, J. and Yliruusi, J. (2006). Monitoring tablet surface roughness during the film coating process. *AAPS Pharm. Sci. Tech.*, 7, 31.

Tomba, E., Barolo, M., and García-Muñoz, S. (2012). General framework for latent variable model inversion for the design and manufacturing of new products. *Ind. Eng. Chem. Res.*, 51, 12886-12900.

Yu, H., and MacGregor, J.F. (2003). Multivariate image analysis and regression for prediction of coating content and distribution in the production of snack foods. *Chemom. Intell. Lab. Syst.*, 67, 125-144.